Journal of Quantitative Spectroscopy & Radiative Transfer 253 (2020) 107162

Contents lists available at ScienceDirect

Journal of Quantitative Spectroscopy & Radiative Transfer

journal homepage: www.elsevier.com/locate/jqsrt

Introducing the dark sky unit for multi-spectral measurement of the night sky quality with commercial digital cameras

Zoltán Kolláth[a,*], Andrew Cool[b], Andreas Jechow[c,d], Kornél Kolláth[a,e], Dénes Száz[a], Kai Pong Tong[a]

[a] Eötvös Loránd University (ELTE) BDPK, Department of Physics, Szombathely, Hungary
[b] Defence Science & Technology Group Australia
[c] Leibniz-Institute of Freshwater Ecology and Inland Fisheries, Berlin, Germany
[d] GFZ German Research Centre for Geosciences, Potsdam, Germany
[e] Hungarian Meteorological Service, Budapest, Hungary

ARTICLE INFO

Article history:
Received 12 December 2019
Revised 8 June 2020
Accepted 8 June 2020
Available online 11 June 2020

Keywords:
Light pollution
Dark sky quality/radiance
Spectrophotography
Dark sky unit

ABSTRACT

Multi-spectral imaging radiometry of the night sky provides essential information on light pollution (sky-glow) and sky quality. However, due to the different spectral sensitivity of the devices used for light pollution measurement, the comparison of different surveys is not always trivial. In addition to the differences between measurement approaches, there is a strong variation in natural sky radiance due to the changes of airglow. Thus, especially at dark locations, the classical measurement methods (such as Sky Quality Meters) fail to provide consistent results. In this paper, we show how to make better use of the multi-spectral capabilities of commercial digital cameras and show their application for airglow analysis. We further recommend a novel sky quality metric the "Dark Sky Unit", based on an easily usable and SI traceable unit. This unit is a natural choice for consistent, digital camera-based measurements. We also present our camera system calibration methodology for use with the introduced metrics.

1. Introduction

Light pollution is a form of environmental pollution that is increasing annually in area and brightness [1] and that requires reliable techniques for monitoring [2]. Modern commercial digital single lens reflex (DSLR) and mirror-less (MILC) cameras provide a viable opportunity to monitor the quality of the night sky and light pollution [2]. Cameras that are able to save images in raw format can be calibrated to measure the radiance of the sky, and the image converted to false colour that represents the distribution of sky brightness [3–6]. These imaging devices are superior to other techniques such as widely used single channel devices e.g. the Sky Quality Meter (SQM). However, there are still several drawbacks for imaging systems used in light pollution monitoring:

- limited spatial resolution, particularly near the horizon,
- limited multi-spectral functionality,
- a missing SI traceable unit for dark skies.

Most of the results presented in the recent literature are based on all-sky measurements obtained with fish-eye lenses. Usually, these lenses provide the necessary resolution for most of the sky, particularly near zenith. Unfortunately, a single all-sky image lacks the resolution and precision close to the horizon, the region of the sky that is normally most interesting for light pollution research. A simple compromise is to take two or multiple fish-eye images in the vertical plane [7]. However, for the highest precision at dark locations and at clear sky conditions it is preferable to rather use a robotic panorama head with a rectilinear lens on a digital camera. For example, a 24 mm lens on a 35 mm full-frame camera covers the whole sky and some of the ground and environment with 28 individual images taken at different pointing directions with high spatial resolution. Since the large aperture lenses and the sensitivity of the camera make it possible to use 6–10 s exposure times, it is possible to perform all the measurements for a whole sky image in 10–15 min at a given location. This duration includes the setup of the system, in most cases the actual measurement takes only 5 min. The short exposure time provides images with no star tails. In addition, the apparent rotation of the sky is negligible during the measurement. However when higher precision is necessary in

* Corresponding author.
E-mail address: kollath.zoltan@sek.elte.hu (Z. Kolláth).

https://doi.org/10.1016/j.jqsrt.2020.107162

azimuth and elevation of the given pixel, a correction is available based on astrometry. The above mentioned procedure provides a very high spatial resolution together with high accuracy and efficiency.

The existing imaging measurements methods are calibrated by different methods and by different reference targets. Therefore the metric and units used by different groups are quite different. Moreover, the units introduced by most of the applications are not necessarily fully compatible with the standard definitions. It is common to use a standard source or a calibration device with spectral characteristics which differ from the spectral response of the measurement device. DSLR cameras are calibrated by astronomical or standard CIE photometry [8]. The commercial software "Sky Quality Camera" (Euromix, Ljubljana, Slovenia) is calibrated by standard stars, thus relying on the astronomical "V" band (see e.g. [9]). The earlier versions of DiCaLum [5] use calibration data obtained in a laboratory and using photopic luminance measurements. Although the two systems match each other within an accuracy of a few percent, the mismatch of the camera green channel and the spectral sensitivity defined in the photometric systems can result in discrepancies. Both solutions do not yet fully exploit the multispectral capabilities of commercial digital cameras. A more detailed application of DSLR cameras in remote sensing related to artificial light at night is published by Sánchez de Miguel and his coworkers [10].

The interpretation of measurements should also take into consideration the natural changes in the sky radiance. Airglow, the natural emission of the molecules and atoms in the upper atmosphere, is the most important dynamic component of night-sky radiance, especially at places with negligible light pollution. The radiance, spectral distribution and colour are all variable as the different components change independently. Oxygen primarily emits in the green spectral line, while sodium emission occurs in orange.

The Sky Quality Meter (SQM) (e.g. [11]) has a custom filter that does not exactly match any astronomical or photopic band, but has an extra sensitivity at blue wavelengths. Here the filter mismatch related differences compared to other systems is larger and sometimes unpredictable. In addition, the displayed unit is not compatible with the standard astronomical definition of magnitude, since the reference is given by a stellar spectrum which has a different level at different wavelengths. This discrepancy is discussed later in the paper. In the larger surveys, the only consistent measurement method is the CCD camera-based system of the US National Park Service [12]. They used a standard astronomical V filter, and the camera was calibrated based on the same photometric system.

As there are an increasing number of digital camera measurements available for scientific research, it is essential to set up a common standard that is compatible with standards definitions and traceable to SI units. In this paper, we provide a novel recommendation for the metric and the unit to measure night sky brightness and show how to utilize the RGB colour information at dark sites and under the presence of airglow.

2. The spectrum of the night sky and night sky imaging with airglow

A spectral radiance measurement by a spectroradiometer provides complete information about night sky quality at a given direction on the sky. However, spectroradiometers sensitive enough for night sky measurements at dark sky locations are expensive and complicated to operate in field experiments. In addition, it is not yet feasible to collect spectral information for the whole sky in an acceptable time frame. We use these devices for calibration purposes and testing the camera measurements and to provide additional data to whole sky images.

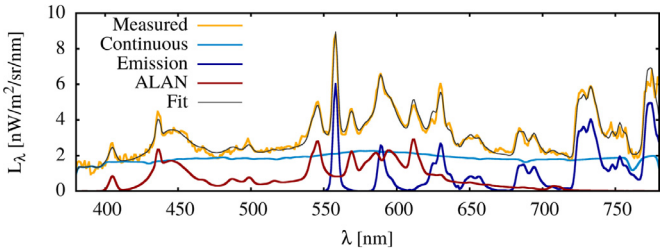

Fig. 1. Typical night sky spectrum at the Zselic Dark Sky Park and its decomposition. The Continuous part is the sum of the zodiacal light, scattered starlight and the residual continuum of the airglow. The ALAN part is the sum of the separately fitted blue and orange part of a white LED spectrum, high-pressure sodium lamp and Compact fluorescent lamp.

Fig. 1 displays the night sky spectrum taken in the Zselic Starry Sky Park in Hungary (coordinates: 46.2366° 17.7653°) on 28.02.2020 at 22:15 UT, western direction, 40° above horizon. The two dominant lines at 558 and 630 nm are the airglow oxygen lines and traces of compact fluorescent lamps and LED's are also visible. A fit with the components of the natural sky spectrum and the typical artificial light sources (blue and orange components of white LED, compact fluorescent lamp, and high-pressure sodium lamp) model the observed spectrum well. The components of the natural spectrum are based on the "Advanced Cerro Paranal Sky Model" [13]. Fig. 1 displays the fit and its major components. The continuous part, which consists of the zodiacal light, scattered starlight and the residual continuum of the airglow, is an approximately flat curve at 2 nW/m^2/sr/nm. We estimated the radiance of the oxygen, sodium and airglow by fitting the airglow models to the two lines. The fitted curve accurately reflects the spectral resolution of the spectroradiometer. The radiance of the lines are $L_{558} = 27$ nW/m^2/sr, $L_{590} = 14$ nW/m^2/sr and $L_{630} = 16$ nW/m^2/sr. The long wavelength OH components sum to $L_{OH} \approx 190$ nW/m^2/sr, which is large compared to the other lines, but has less effect on the digital camera measurements. During the last two years, we have taken several spectral measurements at locations with similar conditions in the Zselic region and these are typical values of the oxygen radiance. A major conclusion from the spectral decomposition is that the continuous part of the natural sky has a flat curve at 2 nW/m^2/sr/nm.

Night sky imaging data at dark locations can be severely affected by airglow. We provide detailed analysis of night sky images in Section 5. Here we refer only to the top left boxes of Figs. 3 and 4. Both measurements were taken in a light-pollution free environment, but for the second time we experienced an intense airglow event. The green oxygen and orange sodium emissions are clearly visible in that image. The comparison of the two all-sky image demonstrates the possible difference due to different airglow activity. However, if one measures the sky brightness only with a monochrome or panchromatic device (e.g. Sky Quality Meter), only the increased level of sky radiance is recognised. Similarly, a naked-eye inspection of the sky showed an increase in background level. Therefore it is necessary to develop measurement methods to determine the real sky quality in the presence of increased airglow. We demonstrate in this paper that digital camera measurements provide an optimal way for this task.

3. What metric and unit(s) to use?

If the spectral response ($S_x(\lambda)$) of a measuring device in a given band 'x' is known, then a well-defined quantity is the band-averaged (spectral) radiance:

$$\bar{L}_x = \int S_x(\lambda) \frac{L(\lambda)d\lambda}{\int S_x(\lambda)d\lambda}; \quad (1)$$

where $L(\lambda)$ is the spectral radiance of the sky at a given direction. If $L(\lambda)$ is a flat (or constant) curve, then the band-averaged radiance is equal to the spectral radiance. Let us denote the output of the measurement device by η_x in the given spectral band 'x'. Then a calibrated (absolute) spectral response curve ($\hat{S}_x(\lambda)$) is defined by the following integral:

$$\eta_x = \int \hat{S}_x(\lambda) L(\lambda) d\lambda; \tag{2}$$

where η_x is the exposure corrected camera raw pixel value. We selected η_x as:

$$\eta_x(k,j) = \frac{DN(k,j) - DN_{\text{black}}}{DN_{\text{satu}} - DN_{\text{black}}} \frac{6400 \times \text{Aperture}^2}{\text{ISO} \times \text{Exposure}}; \tag{3}$$

Where $DN(k, j)$ is the digital number of the (k, j) pixel, DN_{black} and DN_{satu} are the digital numbers of the black and the saturation values of the camera, respectively. Please note that the black level can be replaced by the removal of (multiple, averaged) dark frames, however, according to our experience, the dark frame removal does not increase the precision of the measurements with the modern cameras. Actually, the removal of only a single dark frame increases the noise. For a given sky radiance, η_x has the same order for different cameras - since the cameras are calibrated for correct exposure time. The constant (6400) in the definition of η_x is selected to set the range of the value between zero and the unit, with our standard measurement settings (ISO=3200-6400, the aperture in the order of F/1.4-F/1.8, exposure time a few 1–10 s).

Once $\hat{S}_x(\lambda)$ is measured, the camera is calibrated based on the camera values ($\eta_x(k, j)$) the measured band-averaged radiance is given by:

$$\bar{L}_x(k,j) = \frac{\eta_x(k,j)}{\int \hat{S}_x(\lambda) d\lambda}. \tag{4}$$

Please note that the calibration constant (the denominator integral) can also be given by the maximum value of the spectral response ($S_x(\lambda)$) and the effective width (W_x) of the sensitivity curve:

$$\int \hat{S}_x(\lambda) d\lambda = \hat{S}_x(\lambda_{\max}) W_x; \tag{5}$$

where $W_x = \int S_x(\lambda)/S_x(\lambda_{\max}) d\lambda$. Another choice, especially when a normalised sensitivity curve is used, is to introduce a camera calibration constant: $\int \hat{S}_x(\lambda) d\lambda = C_x \int S_x(\lambda) d\lambda$.

It is important to emphasise that the band-averaged radiance is basically equivalent to spectral density, even if the used filter has a broad spectral band, but giving a mean value over that wavelength range. Therefore the range of the band averaged spectral radiance is independent of the selected color-band or filter. Thus the order of $\bar{L}_x$ is the same as the order of the spectral radiance, as it is a mean value, independent from the effective width of the filter. The natural choice for the unit is nW/m^2/sr/nm. The band-averaged radiance of the natural sky has the order of $\bar{L}_x = 1 - 2$ nW/m^2/sr/nm. As mentioned above, similar values are expected for all the filters (e.g. V) in the visible range. This unit provides a convenient choice, as the cloudy sky at a remote location has a band-averaged radiance about one unit, hence it is the natural choice for light pollution measurements. To shorten the notation, in the following, we will use *dsu* (**Dark Sky Unit**) instead of nW/m^2/sr/nm, which is also equivalent to the SI unit of W/m^2/sr/m, although it is not convenient to measure the wavelength in meters. Please note that NSU (Natural Sky Unit) [14] is already in use, but that unit has an arbitrary zero point with no real SI related or physical meaning. We strongly suggest using our SI traceable unit instead of NSU in future studies related to light pollution.

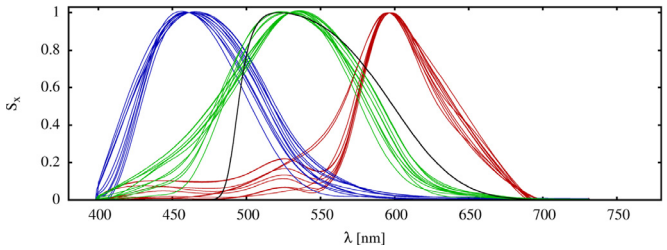

Fig. 2. Typical spectral sensitivity curves of commercial digital cameras with RGB bands. The black line shows the astronomical V band response for comparison.

4. Calibration

An optimal procedure to measure the spectral response is to use a monochromator with a wide-band light source and some high precision (spectro)radiometer, attached together with the camera to an integrating sphere (see e.g. [15]). However, this procedure is not always feasible, especially if one needs to compare a large number of cameras used by activists in light pollution measurements in field conditions. We are using a similar procedure to calibrate selected cameras (details will be published elsewhere). In this paper, we provide a simplified method to compare a larger number of cameras and to make it possible to estimate the error due to the mismatch of spectral response curves.

To provide a quick, but still a reliable comparison of cameras, we tested a simple method based on a series of narrow-band LEDs. The camera sensitivity curves for red, greed and blue (x=R,G,B) channels can be measured in a laboratory, and based on an already calibrated camera, it can be efficiently estimated with a simple measurement sequence. Fig. 2 displays a set of camera sensitivity curves, which are based on a simple measurement technique: A set of narrow-band colour LEDs illuminated a white target with a flat colour response (Microcellular foamed reflector MCPET). At a given measurement, the target was lit only by one LED, and we allowed enough time to eliminate any thermal transients after switching on. The LEDs were driven by a constant DC to avoid any effect by flickering. A Konica-Minolta CS2000A spectroradiometer measured the spectral radiance of the target. At the same time of the spectral measurements, the target was photographed by the selected camera. For camera comparison, we used repeated measurements and when possible, the same lens on different cameras. All the sensitivity curves presented in Figure 2 are based on the above procedure. We collaborated with a local photography club to obtain access to different cameras.

When the absolute camera spectral sensitivity curves are obtained, the camera calibration coefficients can be calculated. However in some cases, when only the relative sensitivity curve is obtained or to increase the precision of the calibration, we use an additional calibration step, preferably at real measurement conditions (typical light level, sky spectrum and camera settings). The spectrum of a spot of the sky where the digital camera image is taken is measured. Based on the relative spectral sensitivity of the camera, the true (spectroradiometer based) band-averaged radiance of the sky in the R,G,B band is calculated and the calibration coefficient is fitted to a set of measurements.

5. Analysis of airglow at dark locations

5.1. Dark locations in Canada without and USA with airglow

Here, we compare the measurement results at two locations (40 km West from Timmins, Ontario, Canada and the Cosmic Campground Dark Sky Sanctuary in New Mexico, USA). At both locations, the light pollution is negligible, and no significant city

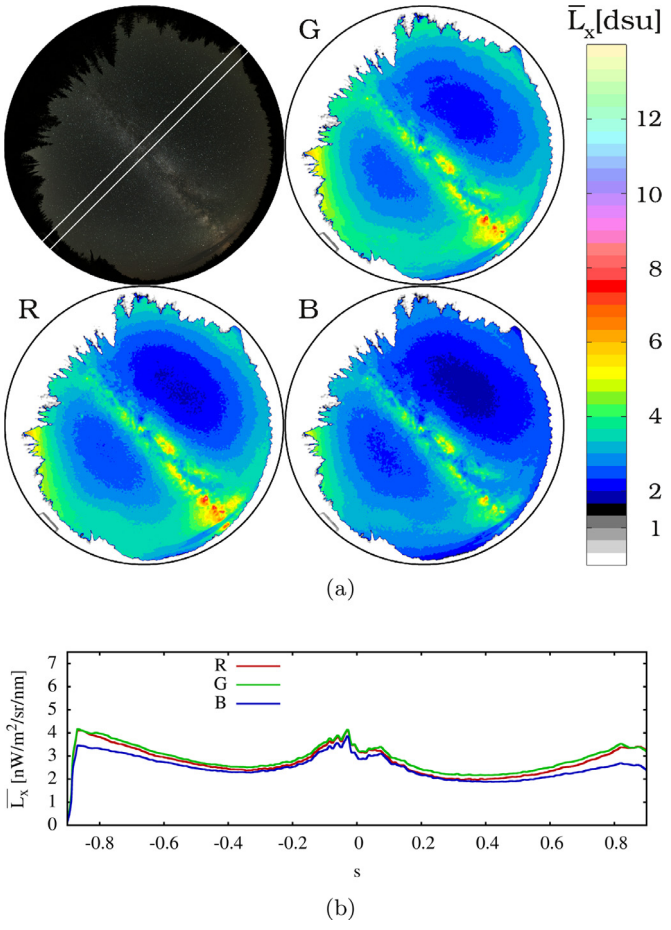

Fig. 3. Real colour image of the natural night sky at a location in Canada with negligible airglow (top left) and the false colour radiance maps of the RGB channels. The variation of $\overline{L_x}$ along a line indicated at the top left image is displayed on the lower panel. Here s is a normalized coordinate on the all-sky image, $\pm$ 1 indicates the horizon, e.g. 90° zenith distance.

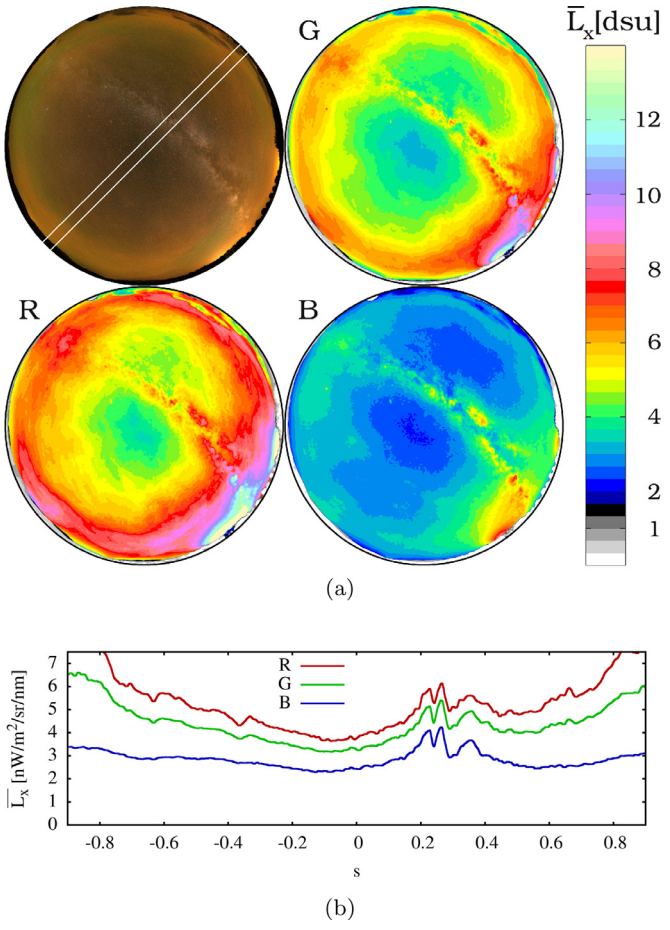

Fig. 4. Real colour image of the natural night sky at Cosmic Campground (top left) The green and red airglow is clearly visible everywhere on the sky. The false colour radiance maps of the RGB channels are displayed in separate panels, the colour channel is indicated by the letter of the colour. The variation of L_x along a line indicated at the top left image is displayed on the lower panel.

light domes are visible at the horizon. However, at the second location, we observed an extreme airglow event.

Fig. 3 displays the results obtained in Ontario Canada (coordinates: 48.4745° -81.7577°) on 25.08.2019 at 04:02 UT. The four boxes show the whole sky image (top left) and the R,G,B band-averaged radiance maps on the same false colour scale. The three channels match each other remarkably well, proving the very low airglow level. The sections of the radiance maps (indicated by white lines on the top left photo) provide a quantitative comparison of the different channels (lower box on the image). Please note, that the modulation due to Milky Way is very similar. This similarity among the three colour channels confirms again that the selected metric is the right choice since at dark locations they have the same level.

Fig. 4 shows the measurement at the Cosmic Campground Dark Sky Sanctuary (coordinates: 33.4796°, -108.9228°) on 20.10.2019 at 03:53 UT. Contrary to the earlier Canadian survey, here we experienced strong airglow. As expected from the colour sensitivity curves of the camera, $\hat{L}_B$ is less affected by airglow than the radiance in the other two colour bands. The section of the radiance maps (lower panel) clearly demonstrates the increased level of airglow.

The difference between the R,G and B channels provides an approximation of the airglow level. The colour information given by the camera's RGB channels makes it possible to estimate the contribution of airglow to the total sky brightness in a more precise way. In the case study presented in this paper, the dominant spectral lines of the airglow are the green (558 nm) oxygen and the orange (589 nm) sodium lines. If we know the relative sensitivity of the colour channels at these lines: $s_x(\lambda_l) = S_x(\lambda_l)/\int S_x(\lambda)d\lambda$ for λ_O = 558 nm, λ_S = 589 nm and for x = R,G,B, then the spectral radiance can be expected in the form:

$$L_x = L_{x,0} + s_x(558) * \xi_{558} + s_x(589) * \xi_{589}, \tag{6}$$

where $L_{x,0}$ is the spectral radiance with no airglow, and ξ_ls are unknown factors to be determined.

Considering our previous result that in the case of low-level airglow, the spectral radiances of the R,G and B channels are very close to each other, we can make an assumption by equaling them. Then we have three unknowns in the above three equations: ξ_ls and $L_0 = L_{R,0} = L_{G,0} = L_{B,0}$. The unknown parameters can be easily calculated from the above equation for each pixel of the whole sky image. Note, that the above assumption is only an approximation, and local features like city light domes, structures in the Milky Way do not follow it.

The left and right panels in Fig. 5 display the results of the above procedure for the data obtained at Cosmic Campground, USA. The left columns show the contribution of the oxygen line to all the colour observations and similarly, the right panels display the same information for the Sodium line. The green airglow component has the expected circular symmetry, and the structure of the red component is clearly displayed.

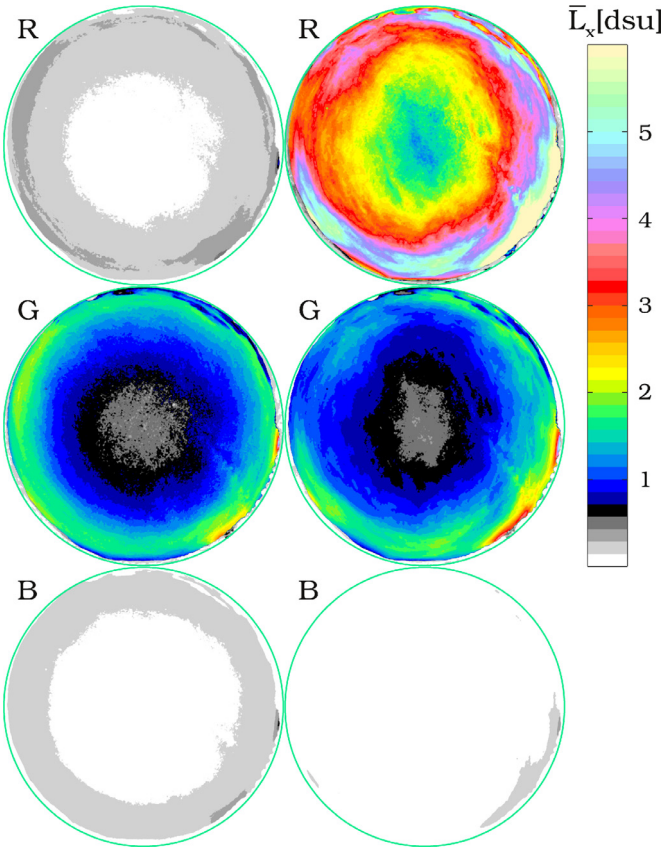

Fig. 5. The contribution of the approximated 558 nm oxygen line (left panels) and the 589 nm sodium line for each colours (indicated by the appropriate letters) for the data obtained at Cosmic campground, USA.

From these results, we can conclude that the sodium airglow mainly affects the red (R) channel and at a lower level the G band. The green oxygen line is present in the G band and negligible in the other two colour channels. The effect of these lines is visible also in the B channel, but at a clearly lower level. Thus, the R-B is a good indicator of the sodium airglow. The ratio of the spectral sensitivity at the two wavelengths in the G band then provides the contribution of sodium line to the green band averaged radiance. Then we can remove the sodium components from the G data and then the difference of the residual G, and the B is a reasonable estimate to the green airglow. The same method applies for the red oxygen line (630 nm), or the combination of the sodium and red lines. For the presented example, this simple estimate gives 1.3*dsu* increase in the red channel by the sodium line and 0.40-0.45*dsu* by the sodium and the 558 nm oxygen line in the green channel, which is in agreement with Fig. 5.

5.2. Other dark locations with minimal airglow

Fig. 6 shows an all-sky image obtained with a DSLR and a fisheye lens (EOS 6D and 8mm Sigma) in the Aralkum desert near Aral Sea in Kazakhstan (coordinates: 46.2623°, 59.8938°) on 27.09.2019 at 15:47 UT. The next settlement was the village of Akbasty in 20 km distance (coordinates: 46.2662°, 60.0978°). The very few lights in the village were sodium lamps with only very few LEDs present. Airglow activity was low with the green (G) channel showing around 2.2 *dsu* and the blue (B) channel about 1.8 *dsu* at the darkest location of the sky. The real colour of the sky as seen in the figure is reddish which is reflected in the 2.5 *dsu* value of the red channel.

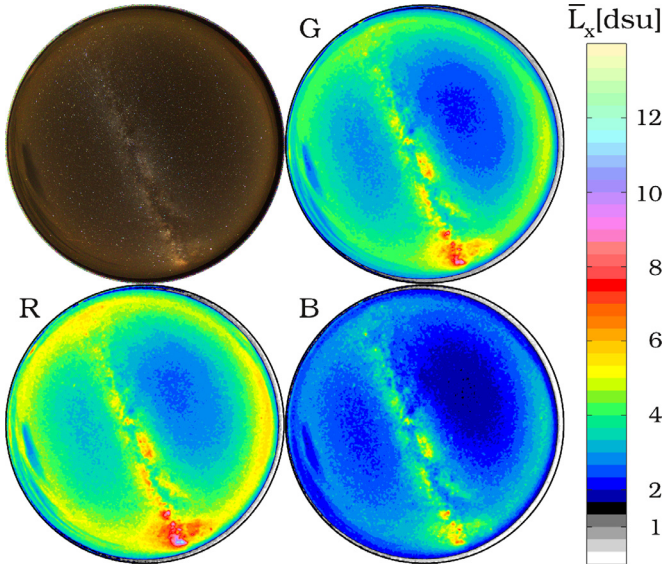

Fig. 6. Real colour image of the natural night sky at location in Kazakhstan with negligible airglow (top left) and the false colour radiance maps of the RGB channels.

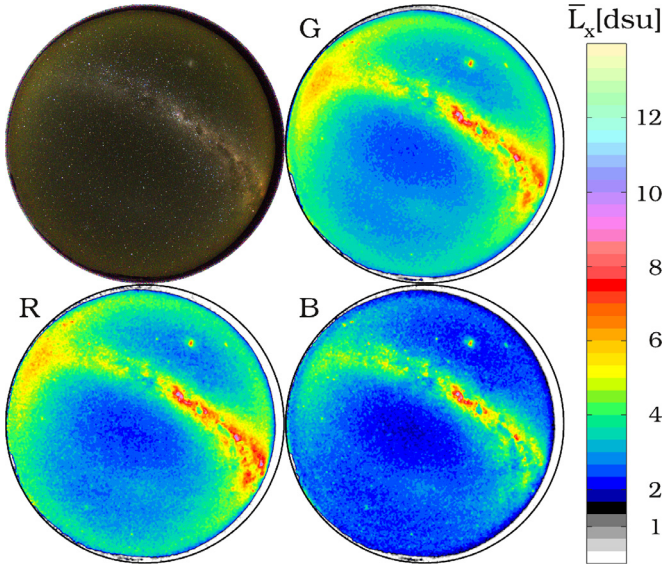

Fig. 7. Real colour image of the natural night sky at location in South Australia (Beltana) with negligible airglow (top left) and the false colour radiance maps of the RGB channels.

Fig. 7 displays an all-sky image obtained with the same type of instrumentation (EOS 6D and 8mm Sigma, ISO 1600 1 min exposure) in Beltana, South Australia (coordinates: -30.3136°, 139.3183°) on 06.04.2019 at 12:52 UT. Airglow activity was low, although here the tone of the real colour image is rather greenish with the green (G) channel showing around 2.3 *dsu* and the red channel showed a lower value (about 2.2 *dsu*).

6. Converting between units and metrics

Our recommended metric is based on the unit of spectral radiance. It would be possible to use the astronomical variant of the unit of spectral irradiance, the jansky (1 Jy = 10^{-26} W m^{-2}Hz^{-1}), to introduce a new measure in Jy/sr or Jy arcsec^{-2}. Please note, however, that transition from *dsu* to Jy/sr requires a wavelength-dependent factor: $L(\lambda)[dsu] = c/\lambda^2 L(\nu)[Jy/sr]$. Since the natural sky has a relatively flat spectral radiance distribution, the mean

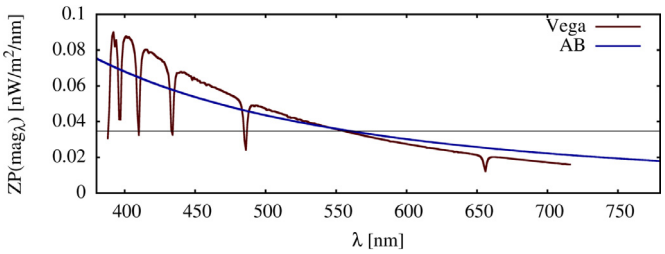

Fig. 8. Spectral reference curves defining the zero point of stellar magnitudes (spectral irradiance of Vega and the absolute magnitude scale).

$L_x[dsu]$ has only a slight variation for the different filters (x). However, then the jansky-based unit has a factor of 2–3 larger values in the blue bands than in the red ones. Therefore it is preferred to use the *dsu* unit over Jy/sr.

The different units used for night sky brightness measurements are related to specific spectral sensitivity. Therefore, any conversion between the units is valid only if it is specified for a given spectrum. Even the frequently used magnitude/arcsecond^2 (mpsas) refers to different absolute radiance when it is based on SQM or astronomical (Johnson) '*V*' band measurements. Thus, any conversion should clearly state the units used and the specific spectral sensitivity.

The digital camera-based measurements are commonly converted to CIE $V(\lambda)$ or astronomical V filter based magnitudes, or to standard photometric (cd/m^2) units. It should be emphasised, that these conversions are only approximations since the camera spectral sensitivity curve is different from these filters. However, since the definition of band-averaged radiance is general for all spectral bands, exact conversion exists for these special filters. For example, if one uses the CIE $V(\lambda)$ filter, then the related $\hat{L}_V$ $[dsu]$ value results in the exact luminance [cd/m^2]: 1 *dsu* in the $V(\lambda)$ band is equivalent to 72.4 μcd /m^2 (this number comes from the 683 lm/watt factor in the photometric definitions and the 106 nm equivalent width of the $V(\lambda)$ filter). Similarly, if we obtain the band-averaged radiance in the Johnson V filter, then it can be converted to standard magnitude/arcsec^2 (mpsas) scale. However, for this conversion, we should use the standard definition of the magnitude scale.

The zero point of the standard astronomical photometry is classically based on a reference spectrum, e.g. the spectral irradiance of Vega (α Lyrae), $E_{\mathrm{Vega}}(\lambda)$. Recently a new 'absolute' (AB) magnitude scale (m_{AB}) is defined by spectral irradiance with a zero point of 3631 Jy [16]. In Fig. 8, the comparison of the reference spectral irradiance definitions is displayed. The frequently used reference point $F_{\lambda=555.6\,nm} = 3.46\,10^{-11}$ W m^{-2} nm^{-1} ([17]) is used to normalize the theoretical spectrum of Vega [18]. A thin horizontal line indicates this reference value in the figure. Note, that the two magnitude scales match each other well at 550 nm, but differ significantly at lower wavelengths. When measuring spectral radiance, the spectral reference is given by $L_{\mathrm{ref}} = E_{\mathrm{ref}}/\Delta\Omega$, where $\Delta\Omega$ is the selected solid angle unit converted to steradians (it is $\Delta\Omega = 2.3504\,10^{-11}$ sr, when the solid angle is measured in square arcseconds).

When the spectral radiance ($L(\lambda)$) is known, then the *dsu* value in a given spectral band can be converted to *mpsas* units based on the following equation:

$$\bar{L}(mpsas) = -2.5\,\log\left(\frac{\int L(\lambda)S_x(\lambda)d\lambda}{\int L_{\mathrm{ref}}(\lambda)S_x(\lambda)d\lambda}\right). \qquad (7)$$

The band-averaged radiance in *dsu* is also given by Eq. (1) Note that this conversion does not depend on the normalization (or absolute calibration) of $S_x(\lambda)$. If the selected filter is the astronomical (Johnson) 'V' band, then an exact conversion is possible: 1 *dsu* in the V_{Bessel} band is equivalent to 22.9 *mpsas*. Please note that this value (and the above mentioned 72.4 μcd/m^2) are coincidentally very close to the sky radiance values obtained under an overcast sky at remote locations (see [19]).

Since 'NSU' is defined to be unit for $L_V = 21.6 mpsas$ for the astronomical V band, the above conversion makes it possible to give a relation between 'NSU' and *dsu*, i.e. 1 NSU is equivalent to 3.4 *dsu*. Here we should mention that any "zero point" defined in the past was arbitrary. The 21.6 *mspsas* value originates in the IAU recommendation ([20]). Later this number was generally used in the literature as quantity for the dark sky (e.g. [21]). The new world atlas of light pollution [22] used 22.0 *mpsas* equivalent to 174 μcd/m^2 and 2.4 *dsu* as a dark limit for the clear sky. Darker sky radiance values were reported recently far from the Milky Way and the zodiacal light. The darkest value we measured during our Canadian survey is 1.8 *dsu* which is equivalent in 'V' band to 22.3 *mpsas* and 130 μcd /m^2.

7. Simulated effects of light pollution sources

To demonstrate the effect of different natural phenomena and the light pollution of the observable quantities we generated a sequence of spectra with different combination of its components. The results are presented in Table 1. The spectra of the natural components are based on the "Advanced Cerro Paranal Sky Model"[1] [13]. We use two extreme models. The low radiance model is calculated at the ecliptic pole, with "Monthly Averaged Solar Radio Flux" of 60 sfu during the middle third of the night in December/January. The effect of moonlight is neglected. We calculated the high radiance model with doubled (120 sfu) radio flux, for April/May conditions. The other parameters are the same. The seasonal change and the increased solar activity provide a significant increase in the natural background (e.g. $\bar{L}_G$ increases from 1.7 *dsu* to 3.1 *dsu*). In the table, we present the theoretical continuous and the emission line contribution separately for the extreme cases.

Based on the low radiance sky model, we constructed a spectral model base on the Cosmic Campground Dark Sky Sanctuary photography measurements. With 1.6 *dsu* continuum level and approximately 100 nW/m^2/sr radiance in the Sodium line and in the green oxygen line, the model reproduces well the RGB measurements. With normal airglow level, this model predicts also the usual sky radiance compatible with the earlier measurements (22.1 mpsas).

We also provide test data by fitting the spectrum obtained in the Zselic Starry Sky Park with the different sources (see Section 2 and Fig. 1). With the spectral decomposition it is possible to list the contribution of all the components. For comparison we added the values calculated from a spectral measurements in a mid size city (Kaposvár, Hungary, coordinates: 46.368020°, 17.785944°)

As expected, the blue camera channel is less affected by the airglow, and the blue radiance provides a good indicator on sky quality in the presence of extreme airglow activity.

The effect of different light sources reflected in the night sky radiance are estimated in our second test. Here we used our spectral data bank to simulate the dependence of the measured R,G,B band-averaged radiance on the correlated colour temperature (CCT). Fig. 9 displays the tendencies and also the camera-related scatter. The green and blue curves have a scatter between $\sigma \approx 1-2\%$ and in the R band it is increased to $\sigma \approx 3\%$. The above error estimates cover only the differences between the sensitivity curves of the different cameras. Please note, however, that if the

[1] https://www.eso.org/sci/software/pipelines/skytools/skymodel.

Table 1
Comparison of the *dsu* values with different filters and for different source spectra. The Cerro Paranal Sky Model was calculated with radio flux of 60 sfu ([a]) and 120 sfu ([b]).

No	Source	$\bar{L}_R[dsu]$	$\bar{L}_G[dsu]$	$\bar{L}_B[dsu]$	$\bar{L}_{V,\mathrm{CIE}}[dsu]$	$\bar{L}_V[dsu]$	$\bar{L}_{\mathrm{SQM}}[dsu]$	$L[\mu cd/m^2]$	mpsas_V
-	Paranal low [a]								
1	Total	1.9	1.7	1.5	1.8	1.7	1.6	132	22.3
2	Continuous	1.4	1.4	1.4	1.5	1.4	1.4	106	22.5
3	Emission	0.4	0.2	0.06	0.4	0.3	0.2	26	-
-	Paranal High [b]								
4	Total	3.4	3.1	2.4	3.5	3.3	2.9	256	21.6
5	Continuous	2.5	2.4	2.3	2.5	2.4	2.4	179	22.0
6	Emission	1.0	0.7	0.2	1.0	0.9	0.6	76	-
7	Cosmic CG Model	3.5	3.1	2.0	3.7	3.4	2.8	270	21.6
-	Zselic								
8	Measured	3.8	3.3	2.7	3.8	3.6	3.1	275	21.5
9	ALAN	1.3	1.0	0.8	1.2	1.1	1.0	91	-
10	Continuous	2.0	2.0	1.8	2.0	2.0	1.9	149	22.2
11	Emission	0.5	0.3	0.04	0.5	0.4	0.3	35	-
12	Natural	2.6	2.3	1.9	2.5	2.4	2.1	184	22.0
13	O(558)	0.04	0.20	0.03	0.25	0.23	0.13	18.2	-
14	Na(590)	0.23	0.08	0.01	0.13	0.11	0.07	9.6	-
15	O(630)	0.20	0.02	0.00	0.08	0.06	0.04	5.7	-
16	OH($>$ 650)	0.06	0.01	0.00	0.01	0.01	0.01	0.9	-
17	Kaposvár	41	32	22	40	37	29	2890	19.0

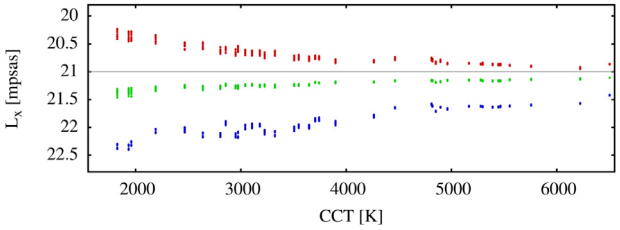

Fig. 9. The effect of different light pollution sources on the sky radiance in different spectral bands. The red, green and blue lines show the variation of the radiance in the R,G,B channels respectively. The gray horizontal line shows the constant reference level in astronomical V band.

cameras are calibrated based on astronomical V band observations, then the camera R, G, B channels varies with the colour temperature in a larger extent. This gives a more than 0.5 mpsas shift in the channels, which can introduce problems if misinterpreted the measurements. That is a major reason to keep the camera-based band-averaged radiances as primary measures.

8. Discussion

Our data shows that the multi-spectral imaging radiometry of the night sky provides significant additional information compared to single-channel measurements. It is especially important when airglow significantly increases sky brightness. When no significant artificial light domes are present on the horizon, e.g. the observer is far from artificial sources, the increased level of sky radiance is the signature of airglow, and whole sky radiance maps can help in the estimation of the airglow level.

Furthermore, even in the presence of artificial light several peculiarities of airglow could enable multi-spectral imaging radiometry with commercial digital cameras to disentangle airglow from skyglow. Airglow should vary on shorter time-scales and may be very different from night to night. Skyglow on the other hand will be rather constant or follow certain user patterns like switching off during the night, at least for perfect clear sky conditions assuming constant atmospheric scattering and attenuation. Furthermore, artificial light could be switched off at town or city scale providing a clear signal at a known time [6].

Based on the normalization of the spectrum of Vega used in this paper, which results in 1 dsu_V equivalent to 22.92 mpsas, and the conversion from *dsu* to cd/m^2 we arrive at the formula between luminance and the magnitude-based scale as

$$L[cd/m^2] = 10.710^4 \times 10^{-0.4L[mpsas]}, \quad (8)$$

which is compatible with the published Vega based conversions. However, this conversion is valid only if the band-averaged radiance is the same with the CIE *V* and in the Bessel *V* filters, since the two metrics depends on those filters. In the examples presented in Table 1. there is a difference between the two spectral radiances in the order of 1–10%. It means that the above formula is valid only by the same precision. The deviation increases further if one uses the SQM for measurements, it can reach 20–30%, error in the conversion. The spectral sensitivity of SQM is different from the Bessel V filter; it has an extra sensitivity in the lower wavelength range. When it is calibrated at the manufacturer, the zero point is determined for a given standard light source. The SQM value is matching the astronomical V measurement only if the spectral distribution of the measured source is similar to that of the standard source. The simulated data used for Table 1 makes it possible to estimate the effect of the spectral mismatch. If we set the zero point of the SQM so that the measurement matches the Bessel V magnitude-based value, then the SQM measures 0.2 mpsas fainter value with the conditions given at the Cosmic Campground measurements. These results are compatible with the conclusion of [23], the SQM measurements have to be interpreted carefully when comparing different sites with different lighting conditions.

There are some other units used in the literature, especially for specialised fields. A widely used unit of spectral irradiance is jansky (Jy) and its derived quantities. It is primarily used in radio astronomy, but any metrics related to spectral densities can be expressed in janskys. The definition of the unit is 1Jy = 10^{-26} W/m^2/Hz, thus Jy/sr or Jy/arcsec^2 can be used instead of *dsu*. However, to the $1/\lambda^2$ conversion from the 1/Hz metric to the 1/nm spectral density normalisation adds a strong wavelength dependence to the otherwise flat spectral radiance curve of the continuous component of the natural sky. That is why our primary preference is to use the *dsu* unit. For reference, we give the conversion rate at 550nm: 1 Jy/sr = 9.91 10^{-15} W/m^2/sr/nm, or 1 μJy/sr = 9.91 nW/m^2/sr/nm.

Another unit defined for the measurements of the radiance of the sky (especially for auroras) is the rayleigh [24] (R) : 1 R = 10^{10} photons/m^2/sr. It is defined for the total radiance of a given au-

rora or airglow line. Again, due to the $1/\lambda$ dependence of photon energy, the conversion factor depends on wavelength. At 558nm (oxygen line), the conversion rate is: 1 R = 0.2833 nW/m^2/sr. As an example: the fitted radiance of the green oxygen airglow line to the Zselic Starry Sky Park measurements (row 13 in Table 1.) is $L_{558} = 27$ nW/m^2/sr, which is equivalent to 95 Raleighs.

The spectral measurement of the night sky makes it possible to calculate the approximate decomposition of the night sky spectral radiance for its main parts. It is possible thanks to the different spectral lines and bands of the natural and artificial components (a vital exemption is the 589 nm sodium line). We can also approximate the airglow components from the RGB images at locations where the artificial contamination is negligible. On the other hand, the spatio-temporal variation of airglow is different from that of the distribution of the artificial light at night. That makes an additional possibility to separate different sources.

9. Conclusion

In this paper, we present a new recommendation for a metric and its unit for dark sky quality measurements. The system is SI traceable and can be implemented by using digital cameras.

- Single-channel measurements do not provide significant information about the quality of the night sky, especially at dark places and in the presence of airglow. Thus measurements only by SQM or similar panchromatic devices can be misleading.
- Digital camera-based three colour radiance measurements give an optimal way for sky brightness measurements. DSLR and MILC cameras are also portable, easy to use at remote locations. With the recent development of imaging optics on mobile devices, they may potentially be used in a similar fashion, while still surpassing panchromatic instruments in terms of spectral information and measurement accuracy.
- It is recommended to use band-averaged radiance as a primary measure of night sky quality. The natural unit is nW/m^2/sr/nm which can be shortened to *dsu*. The difference between the spectral sensitivity of different brands of cameras introduces some error, but it is acceptable when compared to natural changes of night sky radiance.
- No exact conversion is possible from a single band radiance (R_x) values to photopic or astronomical magnitude scales. Based on the colour information, it is possible to estimate the V band radiance, but the error of approximated L_V is still large.

The band-average radiance map of the night sky for the R,G,B channels together provide reliable information on sky quality. A database with digital camera calibration data is under construction. We will provide the necessary information and an open version of the software DiCaLum to promote the use of the recommended metrics and unit.

Declaration of Competing Interest

The authors declare that they have no known competing financial interests or personal relationships that could have appeared to influence the work reported in this paper.

Acknowledgements

This project is supported by the European Union and co-financed by the European Social Fund (Grant no. EFOP–3.6.2–16–201–00014: Development of international research environment for light pollution studies). Andreas Jechow was supported by the Leibniz Association via CONNECT (SAW-K45/2017) and ILES (SAW-2015-IGB-1) projects and the Leibniz-Institute of Freshwater Ecology and Inland Fisheries, via the Frontiers in Freshwater Science project (IGB Frontiers 2017). Andreas Jechow would like to thank Igor Goncharenko who helped during the night sky survey in Kazakhstan and passed away recently at young age.

References

[1] Kyba CCM, Kuester T, Sánchez de Miguel A, Baugh K, Jechow A, Hölker F, et al. Artificially lit surface of earth at night increasing in radiance and extent. Sci Adv 2017;3(11):e1701528. doi:10.1126/sciadv.1701528.
[2] Hänel A, Posch T, Ribas SJ, Aubé M, Duriscoe D, Jechow A, et al. Measuring night sky brightness: methods and challenges. J Quant Spectrosc Radiat Transf 2018;205:278–90. doi:10.1016/j.jqsrt.2017.09.008.
[3] Kolláth Z. Measuring and modelling light pollution at the zselic starry sky park. J Phys Conf Ser 2010;218(1):12001. doi:10.1088/1742-6596/218/1/012001.
[4] Kolláth Z, Dömény A, Kolláth K, Nagy B. Qualifying lighting remodelling in a hungarian city based on light pollution effects. J Quant Spectrosc Radiat Transf 2016;181:46–51. doi:10.1016/j.jqsrt.2016.02.025.
[5] Kolláth Z, Dömény A. Night sky quality monitoring in existing and planned dark sky parks by digital cameras. Int J Sustain Ligh 2017;19(1):61–8. doi:10.26607/ijsl.v19i1.70.
[6] Jechow A, Ribas SJ, Domingo RC, Hölker F, Kolláth Z, Kyba CCM. Tracking the dynamics of skyglow with differential photometry using a digital camera with fisheye lens. J Quant Spectrosc Radiat Transf. 2018;209:212–23. doi:10.1016/j.jqsrt.2018.01.032.
[7] Jechow A, Kyba CCM, Hölker F. Beyond all-sky: assessing ecological light pollution using multi-spectral full-sphere fisheye lens imaging. J. Imaging 2019;5(4):46. doi:10.3390/jimaging5040046.
[8] CIE ISO23539:2005(E)/ CIE S 010/E:2004. Photometry – the CIE system of physical photometry. Standard; CIE; Vienna, Austria; 2005.
[9] Bessell MS. Standard photometric systems. Annu Rev Astron Astrophys 2005;43(1):293–336. doi:10.1146/annurev.astro.41.082801.100251.
[10] Sánchez de Miguel A, Kyba CCM, Aubé M, Zamorano J, Cardiel N, Tapia C, et al. Colour remote sensing of the impact of artificial light at night (i): the potential of the international space station and other DSLR-based platforms. Remote Sens Environ 2019;224:92–103. doi:10.1016/j.rse.2019.01.035.
[11] Cinzano P. Night sky photometry with sky quality meter. ISTIL Int Rep 2005;9:1–14.
[12] Duriscoe DM, Luginbuhl CB, Moore CA. Measuring nightsky brightness with a WideField CCD camera. Publ Astron Soc Pac 2007;119(852):192. doi:10.1086/512069.
[13] Noll S, Kausch W, Barden M, Jones AM, Szyszka C, Kimeswenger S, et al. An atmospheric radiation model for Cerro Paranal: i. The optical spectral range.. Astron Astrophys 2012;543:A92. doi:10.1051/0004-6361/201219040.
[14] Kyba CCM, Tong KP, Bennie J, Birriel I, Birriel JJ, Cool A, et al. Worldwide variations in artificial skyglow. Sci Rep 2015;5:8409. doi:10.1038/srep08409.
[15] Darrodi MM, Finlayson G, Goodman T, Mackiewicz M. Reference data set for camera spectral sensitivity estimation. J Opt Soc Am A 2015;32(3):381–91. doi:10.1364/josaa.32.000381.
[16] Oke JB, Gunn JE. Secondary standard stars for absolute spectrophotometry. Astrophys J 1983;266:713. doi:10.1086/160817.
[17] Megessier C. Accuracy of the astrophysical absolute flux calibrations: visible and near-infrared. Astron Astrophys 1995;296:771.
[18] Takeda Y, Kawanomoto S, Ohishi N. High-Resolution and High-S/N spectrum atlas of vega. Publ Astron Soc Jpn 2007;59(1):245–61. doi:10.1093/pasj/59.1.245.
[19] Jechow A, Hölker F, Kyba CCM. Using all-sky differential photometry to investigate how nocturnal clouds darken the night sky in rural areas. Sci Rep 2019;9(1):1391. doi:10.1038/s41598-018-37817-8.
[20] Cayrel R. 50. Identification and protection of existing and potential observatory sites. Trans Int AstronUnion 1979;17(1):215–23. doi:10.1017/s0251107x00010798.
[21] Cinzano P, Elvidge CD. Night sky brightness at sites from DMSPOLS satellite measurements. Mon Not R Astron Soc 2004;353(4):1107–16. doi:10.1111/j.1365-2966.2004.08132.x.
[22] Falchi F, Cinzano P, Duriscoe D, Kyba CCM, Elvidge CD, Baugh K, et al. The new world atlas of artificial night sky brightness. Sci Adv 2016;2(6):e1600377. doi:10.1126/sciadv.1600377.
[23] Sánchez de Miguel A, Aubé M, Zamorano J, Kocifaj M, Roby J, Tapia C. Sky quality meter measurements in a colour-changing world. Mon Not R Astron Soc 2017;467(3):2966–79. doi:10.1093/mnras/stx145.
[24] Baker DJ. Rayleigh, the unit for light radiance. Appl Opt 1974;13(9):2160–3. doi:10.1364/AO.13.002160.